npj | Climate and Atmospheric Science

www.nature.com/npjclimatsci

ARTICLE OPEN

Aerosol mixing state revealed by transmission electron microscopy pertaining to cloud formation and human airway deposition

Joseph Ching[1], Kouji Adachi[1], Yuji Zaizen[1], Yasuhito Igarashi[2,4] and Mizuo Kajino[1,3]

Aerosol mixing state is one of the most important factors determining the impacts of aerosol particles on aerosol-cloud-climate interactions and human health. The size, composition, and morphology of about 32,000 single particles are analyzed using transmission electron microscopy (TEM) to evaluate per-particle mixing state. Based on the TEM analysis, we quantify aerosol mixing state and examine the impacts of per-particle mixing state on cloud condensation nuclei (CCN) properties and particle deposition efficiency along the human respiratory tract. Assuming homogeneous chemical composition across the aerosol population, a common practice in many global and regional models to various extents, we show that such simplification of mixing state representation could potentially lead to remarkable errors, a maximum of about 90% and 35%, in CCN concentrations and deposition efficiency calculations respectively. Our results from ambient per-particle observations highlight the importance of considering aerosol mixing state in both air quality models and climate models.

npj Climate and Atmospheric Science (2019)2:22 ; https://doi.org/10.1038/s41612-019-0081-9

INTRODUCTION

Aerosol particles play multiple important roles in the atmosphere. From the climate aspect, they can act as cloud condensation nuclei (CCN) and ice nuclei (IN) and scatter and absorb solar and terrestrial radiation, resulting in changing the Earth energy budget directly and indirectly.[1–5] From the human health aspect, particulate matters from local emission, regional scale and long-range transport deteriorate air quality[6,7] and are blamed for increasing incidence of cardiovascular diseases and mortality rate.[8–10] These impacts depend on the aerosol physicochemical properties, which require detailed studies (i) to reduce the uncertainty in aerosol-cloud-climate interactions, one of the largest uncertainties in climate projection;[5,11] and (ii) to understand the various aerosol impacts on human health.[12–14] Numerous studies of laboratory experiments, field observations, and model simulations have examined aerosols to understand their fundamental properties, atmospheric transformation and impacts on climate and human health.

In recent decades, representations of aerosol physicochemical properties in regional and global models have been improved.[15–23] Nevertheless, due to computational constraint, these model representations have been unavoidably simplified to certain degrees and may lead to erroneous calculations of climate-relevant quantities to various extents. On the other hand, more explicit representations of aerosol physicochemical properties and simulations of aerosol atmospheric processing have been conducted in process level modeling frameworks[24–30] to evaluate the impacts of aerosols on climate-relevant quantities. Curtis et al.,[31] developed particle-resolved aerosol representation in single column mode of WRF-Chem meteorology-chemistry coupled model to simulate vertical distribution of mixing state. Recently, Ching and Kajino[14] evaluated the mixing state impact on particle deposition efficiency in the human respiratory tract by developing particle-resolved deposition model.

Regarding measurement techniques, with advancements of single particle analysis instrumentations in recent decades, such as single particle mass spectrometry, scanning transmission X-ray microscopy (STXM), scanning electron microscopy (SEM) and transmission electron microscopy (TEM), atmospheric aerosol is examined in detail at an individual particle level.[32–38] These studies are summarized in Supplementary TC 1. Most of the previous single particle studies categorized aerosol populations into groups by using statistical methods based on dominant chemical compositions and/or by attributing to emission sources and atmospheric transports. More than those, single particle measurements could contribute to the research about aerosol impacts on air quality and climate system. Figure 1 shows how TEM could play a role in the air quality and regional climate research following measurement-to-modeling approach. In terms of climate relevancy, aerosol physicochemical properties determine how particles (i) aid cloud droplets formation, (ii) interact with solar radiation and terrestrial radiation (not shown in Fig. 1); and in terms of air-quality relevancy, how efficiently particles (i) deposit along the human airway after inhalation and (ii) interact with human cells, and the associated toxicity (not shown in Fig. 1). With per-particle physicochemical properties provided by TEM, regional climate and air quality models can be evaluated and further developed to enhance predictive understanding of these aerosol impacts.

[1]Meteorological Research Institute, 1-1 Nagamine, Tsukuba, Ibaraki 305-0052, Japan; [2]Ibaraki University, 2-1-1 Bunkyo, Mito, Ibaraki 310-8512, Japan; [3]Tsukuba University, 1-1-1 Tennodai, Tsukuba, Ibaraki 305-8577, Japan; [4]Present address: Division of Nuclear Engineering Science, Institute for Integrated Radiation and Nuclear Science, Kyoto University (KURNS), 2, Asashiro-Nishi, Kumatori-cho, Sennan-gun, Osaka 590-0494, Japan
Correspondence: Joseph Ching (jching@mri-jma.go.jp) or Kouji Adachi (adachik@mri-jma.go.jp)

Received: 28 February 2019 Accepted: 27 June 2019
Published online: 11 July 2019

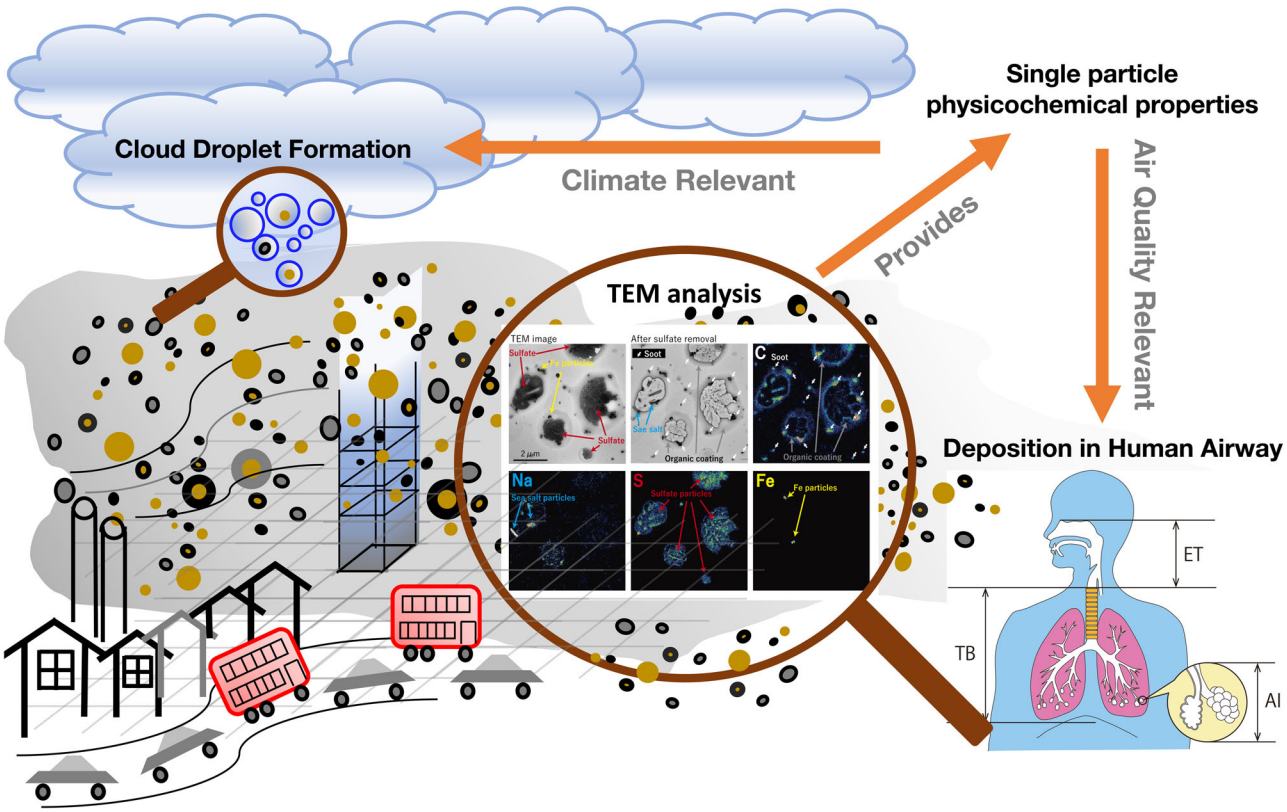

Fig. 1 Schematic showing aerosol mixing state impacts on climate and air quality and role of transmission electron microscopy (TEM) in the corresponding research. Aerosol mixing state determines a number of air-quality-relevant and climate-relevant properties. TEM provides detailed per-particle physicochemical properties, including aerosol mixing state, could contribute to the evaluation and development of air quality and regional models. The illustration of human respiratory system on the bottom right corner is adapted, without any modification, from the Fig. 1 in Ching and Kajino[14] [https://doi.org/10.1038/s41598-018-27156-z] with the permission to use under Attribution 4.0 International (CC BY 4.0)

TEM measures a number of physicochemical properties including particle size, morphology, chemical composition, crystallinity, thermal volatility, and mixing state. This study focuses on aerosol mixing state and on its impacts for cloud droplet formation and deposition efficiency in human airway and takes the first step in the measurement-to-modeling approach. The current study is based on TEM analyzed aerosol properties, endeavors to characterize aerosol mixing state quantitatively by applying the mixing state index[39] and compute mixing-state-dependent CCN properties and deposition efficiency in the human respiratory tract after inhalation. In this study, we use compositions and sizes of about 32,000 aerosol particles measured using TEM, most of which have been analyzed in previous studies and are saved in our publicly accessible aerosol database (http://metemadb.kir.jp/). These aerosol samples were collected in three different locations of urban, mountain and rural environment in Japan. Other techniques, for example aerosol mass spectrometry (AMS) and hygroscopic tandem differential mobility analyzer (HTDMA), work better for specific measurements such as aerosol composition and hygroscopicity, respectively than TEM. The advantages of TEM are that it can analyze or evaluate these properties all together at individual particle level, which are useful for multiple environmental issues such as climate change, air quality, and human health. Although the TEM technique has limitations such as off-line analysis, limited measurements for volatile materials, and sampling sub-100 nm particles, it still provides unique information especially on mixing state of particles including sulfate, sea salt, organic, and refractory materials. By using archived data from several studies and campaigns, we are able to obtain a large number of individual particles information for the purpose of this study. This study aims to (i) present physicochemical properties of single particles analyzed by TEM; (ii) characterize aerosol mixing state by applying mixing state index; and (iii) examine the impact of mixing state on climate-relevant CCN properties and particles deposition efficiencies in the human respiratory tract.

RESULTS

Characterizing aerosol physicochemical properties

Figure 2a, b shows the particle size and shape factor distributions, respectively, in the urban, mountain, and rural samples. In the urban and mountain samples, most particles are of equivalent circular diameter (ECD) between 100 and 300 nm, while in rural samples, they are between 300 and 400 nm. The size distribution reflects the result of superposition of atmospheric processes including emission, deposition, coagulation among particles and condensation of gaseous species. In all the three locations, their shape factors are between 1 and 1.5, suggesting that most particles are neither spherical (shape factor equal to 1) nor extremely irregular. We calculate the per-particle chemical diversity D_i from the seven species (Supplementary Table 2). The bimodal distributions of D_i peak at about 1.8 and 2.8 (Fig. 2c), which means that each particle composes of mainly two or three chemical species. From the size and composition of individual particles, the hygroscopicity κ is calculated according to Petters and Kreidenweis.[40] Figure 2d shows that the κ distribution is bimodal for all the three locations, representing hygroscopic ($\kappa = 0.5–0.6$) and hydrophobic ($\kappa = 0$) particles. The left column of Fig. 3 shows the bulk

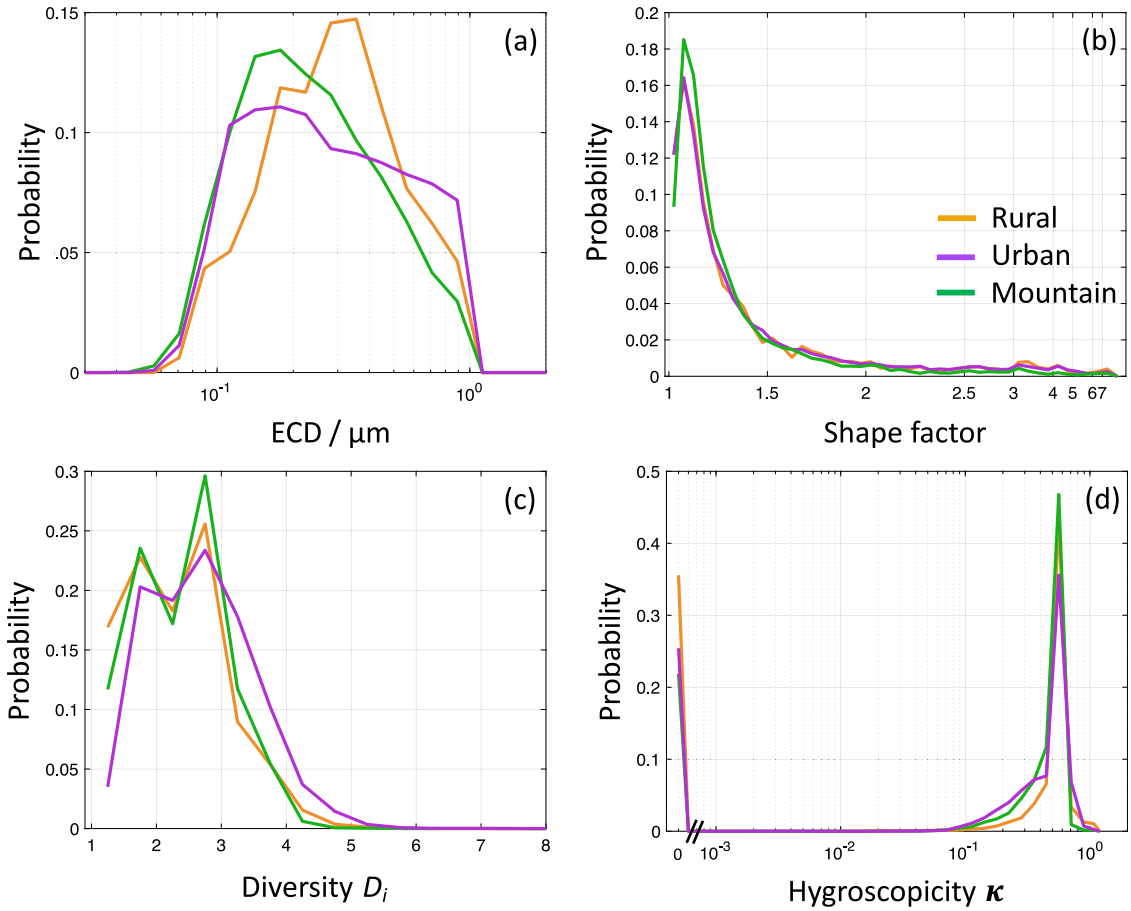

Fig. 2 Normalized probability density functions of various aerosol physicochemical properties. Normalized probability density function of **a** particle equivalent circular diameter (ECD), **b** particle shape factor, **c** per-particle chemical diversity and **d** particle hygroscopicity. Orange, purple and green curves represent rural (Tsukuba), urban (Tokyo) and mountain (Senjyo) respectively

mass fractions of seven species of each particle populations, and the right column shows the corresponding chemical diversities. D_α indicates average number of species in each particle and is equivalent to the particle mass fraction weighted mean of D_i (Fig. 2c) in logarithmic space (Table 2 in[39]). Bulk population species diversity D_γ means the number of species in a population. The D_γ values (Fig. 3b, d, f) are large when there are various colors and each color occupies similar portion in the corresponding bar in Fig. 3a, c, e. On the other hand, for example, the samples principally composed of carbonaceous and sulfate have D_γ around or <2. Figure 4 presents D_α and D_γ of each sample, and the mixing state index χ ($= (D_\alpha - 1)/(D_\gamma - 1)$) and Supplementary Fig. 1 presents the distribution of χ. Most of the urban samples have large χ value (more internally mixed), which is probably due to effective secondary organic aerosol formation and emissions from various sources.[41] Besides, the range of χ shown by rural samples is (3.2%, 31.9%), which is narrower than both urban and mountain samples (Supplementary Fig. 1). The urban samples present a wider range of χ, (2.6%, 81.9%), because the aerosol particles originated from several air mass sources including marine and urban emissions. The mountain samples span a wider range of χ, (10.4%, 71.6%), which is likely due to wide sampling period entailing different modes of interactions among meteorology, emission and chemistry. The rural samples have similar range of D_γ but smaller D_α values than their urban counterparts, which implies that there is more inter-particle diversity in the rural samples. Further model simulations are needed to understand how the rural samples were more externally mixed (smaller χ) than the other two locations.

Impacts of aerosol mixing state on CCN properties and deposition efficiency in the human respiratory tract

The impacts of aerosol mixing state on CCN properties and deposition efficiency after inhalation are evaluated using the approach in Ching et al.[27,42] We compare the CCN fraction and deposition efficiency of each particle population calculated based on our detailed particle mixing state with those based on simplified mixing state representation. The mixing state of a particle population is simplified by assigning each particle identical chemical composition, while preserving its diameter. The identical chemical composition assigned is calculated by averaging volume fractions of the seven species. It should be noted that the bulk volume fractions of the seven species are preserved in this procedure. The details of averaging procedure can be found in *Ching* et al.[27] The hygroscopicity and CCN fraction at environmental supersaturation *SS* are calculated subsequently, denoted by κ_{avg}, and $CCN_{SS,avg}$ respectively. $CCN_{SS,avg}$ is then compared to $CCN_{SS,TEM}$. The difference, ΔCCN, is defined as $(CCN_{SS,avg} - CCN_{SS,TEM})/CCN_{SS,TEM}$. Likewise, we calculate $\Delta F = (F_{z,avg} - F_{z,TEM})/F_{z,TEM}$, where $F_{z,avg}$ is the gross deposition efficiency calculated using formula (1) by replacing the deposition efficiency of particle i, $e_{i,z}$ (D_i, κ_i), with $e_{i,z}$ (D_i, κ_{avg}).

Figure 5 presents the absolute magnitudes of ΔCCN and ΔF, for the sake of focusing on the general pattern between ΔCCN and χ, and between ΔF and χ. Figure 5a shows that $|\Delta CCN|$ ranges from

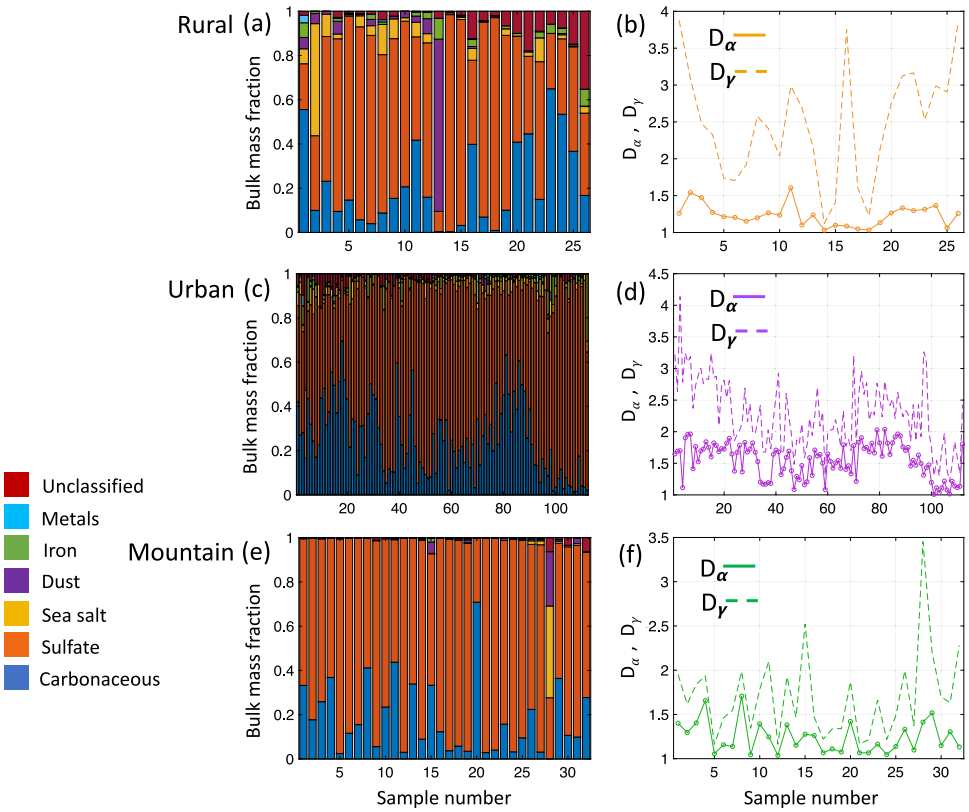

Fig. 3 Mass fractions of seven chemical species and chemical diversity of each sample. Chemical mass fractions in the sample collected in **a** rural (Tsukuba), **c** urban (Tokyo) and **e** mountain (Senjyo) are shown on the left column. The right column shows the corresponding values of average particle species diversity, D_α (solid line with circles) and bulk population species diversity, D_γ (dashed line) in (**b**) rural, (**d**) urban and (**f**) mountain areas respectively

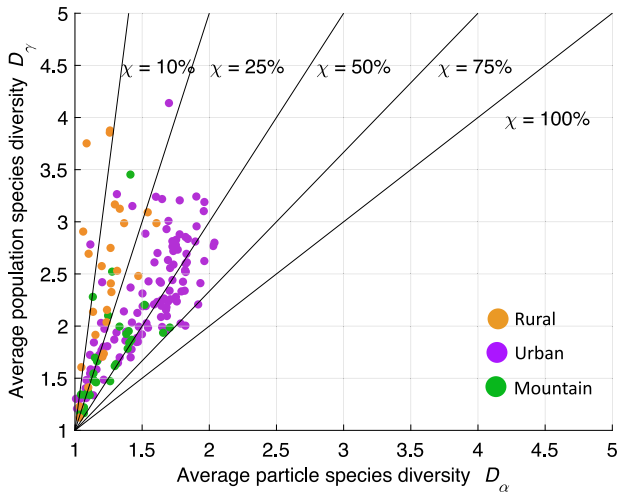

Fig. 4 Scatterplot of average particle species diversity, D_α and bulk population species diversity, D_γ. The solid lines indicate the constant mixing state index χ values. Orange, purple and green filled circles represent rural (Tsukuba), urban (Tokyo) and mountain (Senjyo) respectively

0% to almost 90%, with a decreasing tendency towards large χ value. $|\Delta CCN|$ is attributed only to the simplified mixing state since the particles sizes are preserved in our procedure. Because the populations with large χ have more homogeneous composition, the simplification of mixing state by averaging composition modifies hygroscopicity less significantly for those populations than for populations with smaller χ. The smaller $|\Delta F|$ for the larger χ for adult male doing light exercise (Fig. 5b) is due to the same reason. The mean and mean plus one standard deviation lines in Fig. 5 are computed with assorting χ values into eight bins, each has a width of 10%. Although the solid and dashed lines show a general decreasing trend towards larger χ, there are rises at χ between 55 and 65% for $|\Delta CCN|$ (Fig. 5a), between 30 and 40% and between 55 and 65% for $|\Delta F|$ (Fig. 5b). This is due to the modulation of $|\Delta CCN|$ and $|\Delta F|$ by the underlying particle size distributions, apart from their dependence on χ. Both $|\Delta CCN|$ and $|\Delta F|$ for externally mixed populations (small χ) span a wider range than their counterparts at large χ. This is consistent with the findings in previous particle-resolved modeling study.[42] In short, $|\Delta CCN|$ and $|\Delta F|$ could potentially be large for populations of small χ. In this study, most populations have χ between 40 and 60% (Supplementary Fig. 1), implying that $|\Delta CCN|$ and $|\Delta F|$ could be as large as 60% and greater than 10% respectively depending on other various factors, such as environmental humidity, particle size distribution and location of deposition.

In Fig. 5a, $|\Delta CCN|$ is generally smaller for the higher supersaturations. This is consistent with the reducing impact of mixing state on cloud droplet formation under high environmental supersaturations suggested by Wang et al.,[43] and Ching et al.[42] Since alveolar interstitium (AI) and tracheobronchial airway (TB) are saturated with water vapor, mixing-state-dependent hygroscopic growth of particles occurs, $|\Delta F|$ in AI and TB is sensitive to mixing state, which is consistent with Ching and Kajino.[14] Although the humidity of extrathoracic airway (ET) is in equilibrium with the surrounding environment, which is set at 50% in current study, the mixing state impact on $|\Delta F|$ is also noticeable. Since deposition efficiency in the human respiratory

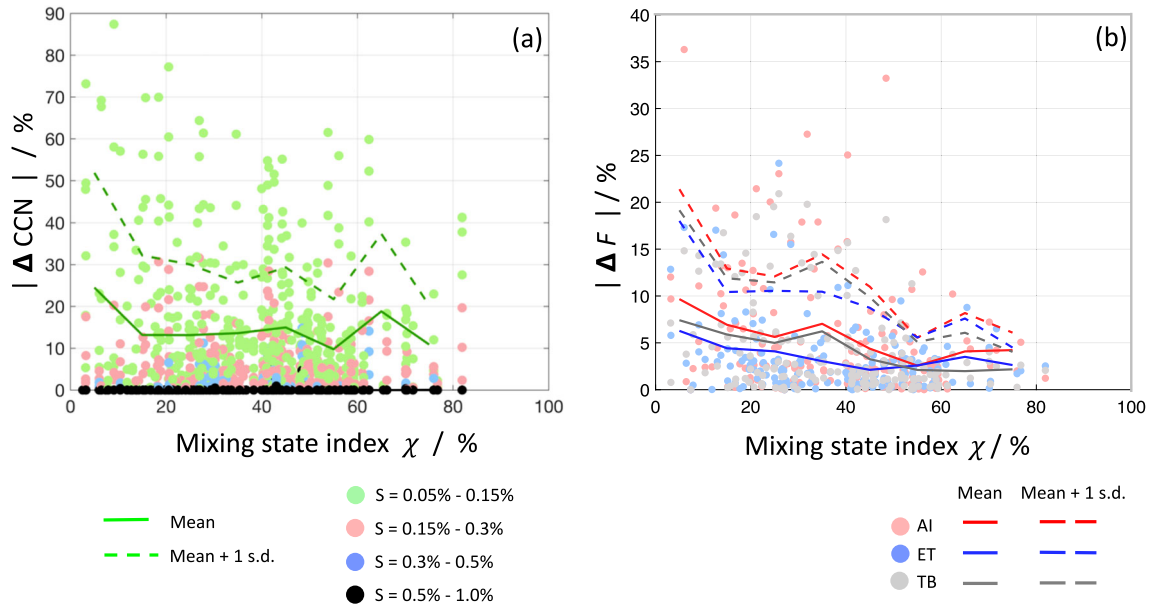

Fig. 5 Error in cloud condensation nuclei, CCN, and particle deposition efficiency, *F* in the human respiratory tract. In **a**, green, red, blue and black filled circles represent environmental supersaturation, *S* ranges of 0.05–0.15, 0.2–0.3 0.35–0.5 and 0.55–1% respectively. In **b**, red, blue and gray filled circles indicate alveolar interstitium (AI), extrathoracic airway (ET) and tracheobronchial airway (TB) of the respiratory tract where the particles deposit respectively. Solid and dashed line indicate the mean and mean plus one standard deviation

tract depends on age, and activity level, we investigate the variation of $|\Delta F|$ with χ for other age and activity level combinations (Supplementary Fig. 2). Patterns in Supplementary Fig. 2 are similar to Fig. 5b, and we conclude that the mixing state impact on deposition efficiency is robust regardless of age and activity level. In addition, we test the robustness of $|\Delta CCN|$ and $|\Delta F|$ to the hygroscopicity (κ) values of sulfate by conducting two sensitivity calculations. One calculation assumes κ of sulfate of 0.5 and the other assumes 0.7, in order to take ammonium nitrate into account (See Supplementary Note 1). The results show that $|\Delta CCN|$ and $|\Delta F|$ do not differ significantly from those calculated assuming κ of sulfate of 0.6 (see Supplementary Figs 2–7).

DISCUSSION

By quantifying the aerosol mixing state in term of χ, this study connects TEM single particle analysis of the ambient samples collected from urban, mountain, and rural sites to the study of aerosol impacts on climate and human health. We calculate the critical supersaturations and deposition efficiencies from the per-particle compositions measured using the TEM analysis. Our results show that urban, mountain, and rural samples encompass a wide range of mixing state and suggest that mixing state simplification could potentially lead to significant error in the calculations of CCN concentrations (maximum error of 90%) and deposition efficiency of inhaled particles (maximum error of 35%). Our results highlight the importance of considering aerosol mixing state in calculating both climate-relevant CCN concentrations, and air-quality-relevant deposition efficiency in human airway.

In the light of the limitations of the current study (see Supplementary Note 1) and continuing the measurement-to-modeling approach (Fig. 1 and Supplementary Fig. 8) to evaluate the mixing state impacts on climate and air quality, from the measurement aspect, we would like to suggest, (i) to carry out more single particle measurements (not limited to TEM), together with size resolved measurements of aerosol and bulk concentration measurement of gaseous pollutants and aerosol in various types of environment. Although large amount of individual particles (about 32,000) from urban, rural and mountain environments are currently analyzed by TEM, more measurements are indispensable to obtain a global picture of aerosol mixing state and asses its deviation from simplified model representations in many climate and air quality models; (ii) to conduct laboratory experiments to determine whether morphology and electric charges of individual particles affect the particle deposition efficiency and their interactions with human tissues. TEM analysis could aid such quantification; and (iii) to conduct interdisciplinary studies between atmospheric scientists and toxicologists to investigate the toxicities of common aerosol particles found in various types of environment and establish a mechanistic understanding of how those particles interact with human cells. By considering aerosol mixing state, atmospheric scientists and epidemiologists can construct a more comprehensive exposure-response function, which describes statistically the human physiological response towards air pollution exposure.

From the modeling aspect, we would like to suggest (i) to further develop existing regional climate and air quality models to represent aerosol physicochemical properties realistically, which is consistent with single particle analyses, since TEM analysis demonstrates that aerosol mixing state treatments in many climate and air quality models are oversimplified; (ii) to simultaneously devote effort to construct computationally efficient aerosol schemes due to limited computational resources. As models are implementing more atmospheric processes, and running in higher and higher spatial resolutions, atmospherically relevant yet computationally efficient aerosol model representations are imperative especially it is a common practice to perform ensemble simulations;[44] and (iii) to evaluate such updated models with single particle measurements collected in a wide range of environments.

Detailed single particle analysis contributes to aerosol model development and evaluation to explore the underlying interplay between emission, meteorology and chemistry governing the physicochemical properties evolutions, the highly uncertain aerosol-cloud-climate interaction and the associated impacts on climate[5,11,45] and air quality.[13,14] This consequently benefits air quality prediction, and pollution mitigation policy devising and aligns with one of the emphases in the theme of sustainable development.[46,47]

METHODS

TEM database of meteorological research institute

Meteorological Research Institute of Japan Meteorological Agency establishes a publicly accessible database of single particles analyzed by TEM, which currently stores physicochemical properties and images of approximately 50,000 individual particles collected in various locations in Japan. Here, we choose the particles of diameter smaller than one micrometer collected from urban, mountain, and rural sites, where locate in Tokyo, Kiso-Komagatake (thereafter Senjyo), and Tsukuba, respectively. Tokyo is one of the largest megacities in the world and is representative of urban environment. The TEM samples from Tokyo used in the current study was analyzed to characterize black carbon mixing states and iron-oxide particles.[41] Senjyo is a mountain site (2611 m above sea level) and has almost no local emission sources near the site (within 8 km). The site is covered by free tropospheric air for much of the time especially during night. The samples have been studied to understand the regional transportation of black carbon particles.[48] Tsukuba is a rural city, which locates ~60 km northeast from Tokyo. The samples were collected at Meteorological Research Institute throughout all seasons. Information about the data analyzed here is given in Supplementary Table 3 and Supplementary Fig. 9.

TEM analysis method

This study measures compositions and shape parameters of individual particles obtained using a transmission electron microscope (JEM-1400, JEOL, Tokyo, Japan) and an energy-dispersive X-ray spectrometer (EDS; X-Max 80, Oxford Instruments, Tokyo, Japan) with scanning-TEM mode (STEM). STEM-EDS data were processed by a software INCA Feature (Oxford Instruments, Tokyo, Japan). Using TEM, we can observe individual particles with hundreds nanometer or less as well as their compositions and mixing states. When observed aerosol particles using TEM, many particles contain several components as coatings, host materials, or inclusions (Supplementary Fig. 10). For example, many sulfate particles have organic coatings and embed nano-metal particles.[49,50] In this study, we evaluate the fractions of materials within individual particles based on the STEM-EDS analysis (Supplementary Fig. 11). This evaluation is challenging because the particles are collected on substrates and contain much light elements (e.g., C and O), which are difficult to quantify using EDS system. In this study, we used assumptions that C signal from carbon substrate correlates to the exposed beam area and all S forms sulfate (SO_4^{2-}). With the recognition of these assumptions and uncertainties, we explore the effects of particle mixing states on CCN properties and deposition efficiency in the respiratory tract. After the data treatments, we quantify the fractions of materials consisting of individual particles into carbonaceous, sulfate, dust, Fe, sea salt, and metal (excluding Fe) followed by the criteria shown in Supplementary Fig. 12. More detailed assumptions and protocol to proceed the particle quantification are discussed in Supplementary Note 2, and Supplementary Figs 10–12.

Chemical diversity and mixing state index

In most model simulations, aerosol mixing states are simply classified using qualitative terms "internally-mixed" and "externally-mixed", which indicate that particles consistent with two or more components or single component, respectively. However, this classification is too simplified in many samples as TEM analyses with elemental image show that most particles have complicated mixing states of various components (Supplementary Fig. 10). Therefore, for more quantitative understanding of the mixing state variations, we apply the chemical diversity and mixing state index proposed by Riemer and West[39] to quantify the mixing state of the aerosol populations. The metrics describe ambient particle mixing states more reasonably and quantitatively and have been applied to quantify the impact of mixing state on various quantities relevant to climate and air quality.[14,29,42] Besides, the index has also been applied in a number of ambient single particle measurement studies[32,34–37] to quantitatively evaluate the mixing state. Detailed mathematical background and physical meaning of the mixing state index are described in Riemer and West.[39] Briefly, the mixing state index, χ, is devised based on the concept of information entropy concerning the distribution of chemical composition across the aerosol population. Mixing state index χ of 0 and 100% indicate completely externally- and completely internally-mixed aerosol population, respectively. However, most ambient particle populations have χ intermediate between 0 and 100%. χ contains information about the average particle level diversity, D_α and population level bulk chemical diversity, D_γ. From the mass fractions of the chemical species classified (Supplementary Fig. 11), we calculate the per-particle diversity, D_i.[39]

CCN concentration and gross deposition efficiency

We calculate the hygroscopicity (κ) of each particle, denoted by κ_i, from the volume fractions weighted mean of hygroscopicity of individual species. The volume fractions are calculated from the mass fractions measured by TEM, assuming respective density values. The κ and density values of each species prescribed in the calculation can be found in Supplementary Table 2. The density of metal (Supplementary Table 2) is calculated according to the mass fractions and densities of Ti, Mn, Ni, Zn, and Pb, which are classified into metal species (Supplementary Fig. 12). From the hygroscopicity of individual particles, we calculate the critical supersaturation according to κ-Köhler theory.[40] Then we determine the ratio of the number of particles activated at supersaturation y to the total number of particle for each sampled population, denoted by $CCN_{SS,\mathrm{TEM}}$. Besides, we evaluate the gross deposition efficiency, denoted by $F_{z,\mathrm{TEM}}$, where z is one of the three locations, AI, ET and TB in the human respiratory tract, according to

$$F_{z,\mathrm{TEM}} = \frac{\sum_{i=1}^{N} e_{i,z}(D_i,\kappa_i)\times A_i \times f_{\mathrm{M},i}}{\sum_{i=1}^{N} A_i \times f_{\mathrm{M},i}}, \quad (1)$$

where A_i is the cross section area and $f_{M,i}$ represents the sum of mass fractions of Ti, V, Cr, Mn, Fe, Ni, Zn and Pb of particle i. $e_{i,Z}$ is the deposition efficiency of particle i at location z. Since the human respiratory tract is saturated (AI and TB) with water vapor, inhaled particles experience hygroscopic growth determined by both particles size D_i and hygroscopicity κ_i. The hygroscopic growth and the deposition efficiency $e_{i,Z}$ are calculated by the deposition model.[14,51] We set the relative humidity of AI and TB as 99% in the current deposition calculation. The humidity of ET is in equilibrium with the surrounding environment, which is set as 50% in this study.

DATA AVAILABILITY

Transmission electron microscopy (TEM) data presented here is available in our publicly accessible aerosol database (http://metemadb.kir.jp/). Other data that support the findings of this study are available from the corresponding author upon reasonable request.

ACKNOWLEDGEMENTS

This research project was mainly supported by the Fundamental Research Budget of MRI (C3, P5, and M5). In addition, we acknowledge the financial support by the Environmental Research and Technology Development Fund (5– 1605 (JC, MK, KA) and 2-1703 (KA)) of the Environmental Restoration and Conservation Agency (ERCA), Japan and the JSPS KAKENHI (grant numbers JP16K16188 (KA) and JP15H02811(YZ, KA)).

AUTHOR CONTRIBUTIONS

J.C. and M.K. designed the study. J.C. performed calculations and data analysis. J.C. and K.A. wrote the manuscript from the input of all the authors. K.A. and Y.Z. performed TEM sample treatment and analysis. Y.I. and M.K. proposed the establishment of the TEM database and provided guidance on the methodology and execution of the study.

ADDITIONAL INFORMATION

Supplementary Information accompanies the paper on the *npj Climate and Atmospheric Science* website (https://doi.org/10.1038/s41612-019-0081-9).

Competing interests: The authors declare no competing interests.

Publisher's note: Springer Nature remains neutral with regard to jurisdictional claims in published maps and institutional affiliations.

REFERENCES

1. Twomey, S. Pollution and the planetary albedo. *Atmos. Environ.* **8**, 1251–1256 (1974).
2. Albrecht, B. A. Aerosols, cloud microphysics, and fractional cloudiness. *Science* **245**, 1227–1230 (1989).
3. Lohmann, U. & Feichter, J. Global indirect aerosol effects: a review. *Atmos. Chem. Phys.* **5**, 715–737 (2005).

4. Haywood, J. & Boucher, O. Estimates of the direct and indirect radiative forcing due to tropospheric aerosols: A review. *Rev. Geophys.* **38**, 513–543 (2000).
5. Seinfeld, J. H. et al. Improving our fundamental understanding of the role of aerosol− cloud interactions in the climate system. *Proc. Natl Acad. Sci. USA* **113**, 5781–5790 (2016).
6. Inomata, Y. et al. Source–receptor relationship analysis of the atmospheric deposition of PAHs subject to long-range transport in Northeast Asia. *Environ. Sci. Technol.* **51**, 7972–7981 (2017).
7. Shrivastava, M. et al. Global long-range transport and lung cancer risk from polycyclic aromatic hydrocarbons shielded by coatings of organic aerosol. *Proc. Natl Acad. Sci. USA* **114**, 1246–1251 (2017).
8. Dockery, D. W. et al. An association between air pollution and mortality in six US cities. *New Engl. J. Med.* **329**, 1753–1759 (1993).
9. Pope, C. A. III Review: epidemiological basis for particulate air pollution health standards. *Aerosol Sci. Technol.* **32**, 4–14 (2000).
10. Pope, C. A. III & Dockery, D. W. Health effects of fine particulate air pollution: lines that connect. *J. Air Waste Manag. Assoc.* **56**, 709–742 (2006).
11. IPCC, 2013: Climate Change 2013: The Physical Science Basis. Contribution of Working Group I to the FifthAssessment Report of the Intergovernmental Panel on Climate Change (eds Stocker, T. F., Qin, D., Plattner, G.-K., Tignor, M., Allen, S. K., Boschung, J., Nauels, A., Xia, Y., Bex, V. and Midgley, P. M.) 1535 (Cambridge University Press, Cambridge, United Kingdom and New York, NY, USA). https://doi.org/10.1017/CBO9781107415324.
12. Kameda, T. et al. Mineral dust aerosols promote the formation of toxic nitropolycyclic aromatic compounds. *Sci. Rep.* **6**, 24427 (2016).
13. Shiraiwa, M. et al. Aerosol health effects from molecular to global scales. *Environ. Sci. Technol.* **51**, 13545–13567 (2017).
14. Ching, J. & Kajino, M. Aerosol mixing state matters for particles deposition in human respiratory system. *Sci. Rep.* **8**, 8864 (2018).
15. Vignati, E., Wilson, J. & Stier, P. M7: an efficient size-resolved aerosol microphysics module for large-scale aerosol transport models. *J. Geophys. Res.* **109**, D22202, https://doi.org/10.1029/2003JD004485 (2004).
16. Stier, P. et al. The aerosol-climate model ECHAM5-HAM. *Atmos. Chem. Phys.* **5**, 1125–1156 (2005).
17. Mann, G. W. et al. Description and evaluation of GLOMAP-mode: a modal global aerosol microphysics model for the UKCA composition-climate model. *Geosci. Model Dev.* **3**, 519–551 (2010).
18. Aquila, V. et al. MADE-in: a new aerosol microphysics submodel for global simulation of insoluble particles and their mixing state. *Geosci. Model Dev.* **4**, 325–355 (2011).
19. Liu, X. et al. Toward a minimal representation of aerosols in climate models: description and evaluation in the Community Atmosphere Model CAM5. *Geosci. Model Dev.* **5**, 709 (2012).
20. Matsui, H. et al. Development and validation of a black carbon mixing state resolved three-dimensional model: aging processes and radiative impact. *J. Geophys. Res.: Atmos.* **118**, 2304–2326 (2013).
21. Matsui, H. Development of a global aerosol model using a two-dimensional sectional method: 1. Model design. *J. Adv. Model. Earth Syst.* **9**, 1921–1947 (2017).
22. Kajino, M. et al. NHM-Chem, the Japan Meteorological Agency's Regional Meteorology-Chemistry Model: Model Evaluations toward the Consistent Predictions of the Chemical, Physical, and Optical Properties of Aerosols, *J. Meteorological Soc. Japan*, 2019-020, https://doi.org/10.2151/jmsj (2018).
23. Kajino, M. et al. NHM-Chem, the Japan Meteorological Agency's regional meteorology – chemistry model (v1.0): model description and aerosol representations, *Geosci. Model Dev. Discuss*. https://doi.org/10.5194/gmd-2018-128 (2018).
24. Riemer, N., West, M., Zaveri, R. A. & Easter, R. C. Simulating the evolution of soot mixing state with a particle-resolved aerosol model. *J. Geophys. Res.* **114**, D09202, https://doi.org/10.1029/2008JD011073 (2009).
25. Oshima, N., Koike, M., Zhang, Y. & Kondo, Y. Aging of black carbon in outflow from anthropogenic sources using a mixing state resolved model: 2. Aerosol optical properties and cloud condensation nuclei activities. *J. Geophys. Res.* **114**, D18202, https://doi.org/10.1029/2008JD011681 (2009).
26. Zaveri, R. A., Barnard, J. C., Easter, R. C., Riemer, N. & Matthew, W. Particle-resolved simulation of aerosol size, composition, mixing state, and the associated optical and cloud condensation nuclei activation properties in an evolving urban plume. *J. Geophys. Res.* **115**, D17210, https://doi.org/10.1029/2009JD013616 (2010).
27. Ching, J., Riemer, N. & West, M. Impacts of black carbon mixing state on black carbon nucleation scavenging: insights from a particle-resolved model. *J. Geophys. Res.* **117**, D23209, https://doi.org/10.1029/2012JD018269 (2012).
28. Ching, J., Riemer, N. & West, M. Black carbon mixing state impacts on cloud microphysical properties: effects of aerosol plume and environmental conditions. *J. Geophys. Res. Atmos.* **121**, 5990–6013 (2016).
29. Ching, J., West, M. & Riemer, N. Quantifying impacts of aerosol mixing state on nucleation-scavenging of black carbon aerosol particles. *Atmosphere* **9**, 17 (2018).
30. Fierce, L., Riemer, N. & Bond, T. C. Explaining variance in black carbon's aging timescale. *Atmos. Chem. Phys.* **15**, 3173–3191 (2015).
31. Curtis, J. H., Nicole, R. & Matthew, W. A single-column particle-resolved model for simulating the vertical distribution of aerosol mixing state: WRF-PartMC-MOSAIC-SCM v1. 0. *Geosci. Model Dev.* **10**, 4057–4079 (2017).
32. Healy, R. M. et al. Single particle diversity and mixing state measurements. *Atmos. Chem. Phys.* **14**, 6289–6299 (2014).
33. Giorio, C. et al. Local and regional components of aerosol in a heavily trafficked street canyon in central London derived from PMF and cluster analysis of single-particle ATOFMS spectra. *Environ. Sci. Technol.* **49**, 3330–3340 (2015).
34. Ye, Q. et al. Spatial variability of sources and mixing state of atmospheric particles in a metropolitan area. *Environ. Sci. Technol.* **52**, 6807–6815 (2018).
35. O'Brien, R. E. et al. Chemical imaging of ambient aerosol particles: observational constraints on mixing state parameterization. *J. Geophys. Res.: Atmos.* **120**, 9591–9605 (2015).
36. Matthew, F. et al. Elemental mixing state of aerosol particles collected in Central Amazonia during GoAmazon2014/15. *Atmosphere* **8**, 173 (2017).
37. Bondy, A. L. et al. The diverse chemical mixing state of aerosol particles in the southeastern United States. *Atmos. Chem. Phys.* **18**, 12595–12612 (2018).
38. Wang, Y. et al. Fractal dimensions and mixing structures of soot particles during atmospheric processing. *Environ. Sci. Technol. Lett.* **4**, 487–493 (2017).
39. Riemer, N. & West, M. Quantifying aerosol mixing state with entropy and diversity measures. *Atmos. Chem. Phys.* **13**, 11423–11439 (2013).
40. Petters, M. D. & Kreidenweis, S. M. A single parameter representation of hygroscopic growth and cloud condensation nucleus activity. *Atmos. Chem. Phys.* **7**, 1961–1971 (2007).
41. Adachi, K., Moteki, N., Kondo, Y. & Igarashi, Y. Mixing states of light-absorbing particles measured using a transmission electron microscope and a single-particle soot photometer in Tokyo, Japan. *J. Geophys. Res.: Atmos.* **121**, 9153–9164 (2016).
42. Ching, J., Fast, J., West, M. & Riemer, N. Metrics to quantify the importance of mixing state for CCN activity. *Atmos. Chem. Phys.* **17**, 7445–7458 (2017).
43. Wang, J., Cubison, M. J., Aiken, A. C., Jimenez, J. L. & Collins, D. R. The importance of aerosol mixing state and size-resolved composition on CCN concentration and the variation of the importance with atmospheric aging of aerosols. *Atmos. Chem. Phys.* **10**, 7267–7283 (2010).
44. Ching, J., Zaveri, R. A., Easter, R. C., Riemer, N. & Fast, J. D. A three-dimensional sectional representation of aerosol mixing state for simulating optical properties and cloud condensation nuclei. *J. Geophys. Res.: Atmos.* **121**, 5912–5929 (2016).
45. Li, W. et al. A conceptual framework for mixing structures in individual aerosol particles. *J. Geophys. Res.: Atmos.* **121**, 13784–13798 (2016).
46. National Academies of Sciences, Engineering, and Medicine. *The Future of Atmospheric Chemistry Research: Remembering Yesterday, Understanding Today, Anticipating Tomorrow*. (The National Academies Press, Washington, DC, 2016).
47. United Nations Department of Economic and Social Affairs, Statistics Division. *The Sustainable Development Goals Report 2018*. https://unstats.un.org/sdgs/files/report/2018/TheSustainableDevelopmentGoalsReport2018-EN.pdf (2018).
48. Adachi, K., Zaizen, Y., Kajino, M. & Igarashi, Y. Mixing state of regionally transported soot particles and the coating effect on their size and shape at a mountain site in Japan. *J. Geophys. Res.: Atmos.* **119**, 5386–5396 (2014).
49. Adachi, K., Chung, S. H. & Buseck, P. R. Shapes of soot aerosol particles and implications for their effects on climate. *J. Geophys. Res.: Atmos.* **115**, D15206 (2010).
50. Adachi, K. & Buseck, P. R. Internally mixed soot, sulfates, and organic matter in aerosol particles from Mexico City. *Atmos. Chem. Phys.* **8**, 6469–6481 (2008).
51. Kajino, M., Igarashi, Y. & Fujitani, Y. Which is more efficiently deposited in the human respiratory tract through inhalation, fresh soot or aged soot? Sensitivity of regional depositions to size distribution and hygroscopicity of aerosols. *J. Jpn. Soc. Atmos. Environ.* **49**, 101–108 (2014).